A finite fracture mechanics model for the prediction of the open-hole strength of composite laminates

Published in:

Document Version:
Peer reviewed version

Queen's University Belfast - Research Portal:
Link to publication record in Queen's University Belfast Research Portal

A finite fracture mechanics model for the prediction of the notched strength of composite laminates

P.P. Camanho [a,*], G.H. Erçin [b], G. Catalanotti [a], S. Mahdi [c], P. Linde [d]

[a]*DEMec, Faculdade de Engenharia, Universidade do Porto, Rua Dr. Roberto Frias, 4200-465, Porto, Portugal*

[b]*INEGI, Instituto de Engenharia Mecânica e Gestão Industrial, Rua Dr. Roberto Frias 400, 4200-465, Porto, Portugal*

[c]*AIRBUS Operations SAS, 316, Route de Bayonne, 31060 Toulouse Cedex 03, France*

[d]*AIRBUS Operations GmbH, Kreetslag 10, 21129 Hamburg, Germany*

Abstract

A new model based on finite fracture mechanics is proposed to predict the open-hole tensile strength of composite laminates. Failure is predicted when both stress-based and energy-based criteria are satisfied. The material properties required by the model are the laminate unnotched strength and fracture toughness. No empirical adjusting parameters are required. Using experimental data obtained in quasi-isotropic carbon-epoxy laminates it is concluded that the model predictions are very accurate, resulting in improvements over the traditional strength prediction methods. It also is shown that the proposed finite fracture mechanics model can be used

to predict the brittleness of different combinations of materials and geometries.

1 Introduction

The aerospace industry strives for accurate, physically-based and fast strength prediction methods for composite laminates with stress concentrations. While the two first conditions can be satisfied using appropriate non-linear finite element (FE) models [1]–[5], the third one cannot. Implicit non-linear FE models that include material instabilities result in severe convergence difficulties and require very fine meshes with element sizes typically smaller than 1mm. The computing time of explicit non-linear FE models is partially defined by the stable time increment that decreases with the element size. Both approaches normally result in long computing times that are not acceptable for preliminary sizing and for the optimization of aircraft structural details.

The most widely used design method for composite laminates with stress concentrations that is suitable for preliminary sizing and optimization is the point stress or the average stress models proposed by Whitney and Nuismer [6], or variations of thereof [7]. The point stress model assumes that failure takes place when the stress at a given distance from the notch boundary (the 'characteristic distance') reaches the unnotched strength of the laminate, whereas the average stress model predicts failure when the average stress over a

---
* Corresponding author
Email address: `pcamanho@fe.up.pt` (P.P. Camanho).

2

characteristic distance is equal to the unnotched strength of the laminate. The characteristic distance must be identified from a test in a notched laminate. While the point or average stress models provides reasonable predictions for hole diameters close to that used for the model calibration, they have one main problem: the 'characteristic distance' is not a material property, it depends on both the material/lay-up and on the geometry [8]. As a result, large and expensive experimental programmes are required to identify the characteristic distances for the different materials and geometries.

An alternative method for the strength prediction of composite laminates loaded in tension containing notches or cracks based on the numerical implementation of cohesive formulations were developed Bäcklund et al. [9]–[12]. The damage mechanisms that occur at the vicinity of a crack or hole are lumped into a damage zone, where a linear relation between the cohesive traction and the crack opening is assumed. A traction-free crack develops when the dissipated energy equals the fracture toughness of the laminate. While this method is based on sound mechanical models, the need for a numerical implementation renders it unsuitable for fast predictions.

Based on the previous observations, the objective of this paper is to develop a fast strength prediction method for composite laminates with circular holes loaded in tension. The strength prediction method should be based on independently measured material properties, and it must not require any type of calibration for different hole sizes or specimen widths.

The model developed is based on the concept of finite fracture mechanics that was originally introduced by Leguillon [13]. Finite fracture mechanics models assume that crack propagation results from the simultaneous fulfilment

44 of a stress-based criterion and an energy-based criterion. In addition, it is

45 considered that failure occurs by the propagation of kinematically admissible

46 cracks with finite sizes.

47 The finite fracture mechanics criteria predict failure based on two conditions

48 [14]: the stress ahead of a crack tip averaged over a distance l reaches the ma-

49 terial strength X_T^L, i.e. $\int_a^{a+l} \sigma(x)dx = X_T^L l$. In addition, the energy available

50 to propagate the crack a finite distance l must be equal to a critical value

51 that is defined by the fracture toughness of the material. This condition, es-

52 tablished using the stress intensity factor $\mathcal{K}$ and its critical value $\mathcal{K}_{Ic}$, reads

53 [14]: $\int_a^{a+l} \mathcal{K}_I^2(a)da = \mathcal{K}_{Ic}^2 l$.

54 Finite fracture mechanics models have been applied to the prediction of frac-

55 ture of unidirectional composites under off-axis tension [15], sharp V-notches

56 in isotropic materials [16]–[17], three-point bending tests in notched and un-

57 notched specimens [14], [18], bi-material joints [19], and free-edge delamination

58 [20].

59 ## 2 Finite fracture mechanics model for notched composites

60 Consider a composite laminate with a central circular hole with a diameter d,

61 radius R and width W loaded in tension (Figure 1).

62 [Fig. 1 about here.]

63 For the loading conditions shown in Figure 1, and assuming that the lay-up

64 of the laminate leads to either the brittle or pull-out failure modes defined

65 by Green et al. [21], the propagation of the macro-crack that leads to final

4

failure occurs along the x-direction. Using the coupled stress and energy finite fracture mechanics criterion proposed by Cornetti et al. [14] for the particular case of a specimen with an uncracked central circular hole, fracture occurs when the following system of equations is satisfied:

$$
\begin{cases}
\frac{1}{l} \int_R^{R+l} \sigma_{yy}(x,0)dx = X_T^L \\
\\
\\
\frac{1}{l} \int_R^{R+l} \mathcal{K}_I^2(a)da = \mathcal{K}_{Ic}^2
\end{cases}
\tag{1}
$$

where X_T^L is the unnotched strength of the laminate, $\mathcal{K}_{Ic}$ is the mode I fracture toughness of the laminate, and l is the crack extension at failure. The first equation in (1) corresponds to the average-stress model [6]; therefore, the proposed finite fracture model enriches the average-stress model using a second equation that represents an energy balance that must be satisfied during crack propagation. Taking into account that the system of equations (1) yields the remote notched strength and the crack extension at failure, there is no need to use an empirical 'characteristic distance' identified from one notched test specimen [6].

The stress distribution along the x-axis, $\sigma_{yy}(x,0)$, is obtained as [22]:

$$
\sigma_{yy}(x,0) = R_K \frac{\sigma^\infty}{2} \left[2 + \xi^2 + 3\xi^4 - (K_T^\infty - 3)\left(5\xi^6 - 7\xi^8\right)\right], \ \xi = \frac{R}{x}
\tag{2}
$$

where σ^∞ is the remote stress, K_T^∞ is the stress concentration factor of an infinite plate containing a circular hole, and R_K is the finite width correction

5

82 factor. These parameters are defined as [22]:

$$K_T^\infty = 1 + \sqrt{\frac{2}{A_{22}}\left(\sqrt{A_{11}A_{22}} - A_{12} + \frac{A_{11}A_{22} - A_{12}^2}{2A_{66}}\right)} \quad (3)$$

$$R_K = \frac{K_T}{K_T^\infty} =$$

$$= \left\{\frac{3\left(1 - 2R/W\right)}{2 + \left(1 - 2R/W\right)^3} + \frac{1}{2}\left(\frac{2R}{W}M\right)^6 (K_T^\infty - 3)\left[1 - \left(\frac{2R}{W}M\right)^2\right]\right\}^{-1} \quad (4)$$

83 where A_{ij} are the components of the laminate in-plane stiffness matrix [24],

84 and M is calculated as:

$$M^2 = \frac{\sqrt{1 - 8\left[\frac{3(1-2R/W)}{2+(1-2R/W)^3} - 1\right]} - 1}{2\left(2R/W\right)^2} \quad (5)$$

85 The stress intensity factor $\mathcal{K}_I$ corresponding to two symmetric cracks emanat-

86 ing from a plate with a central circular hole is given for an isotropic plate as

87 [23]:

$$\mathcal{K}_I = \sigma^\infty F_h F_w \sqrt{\pi a} \quad (6)$$

88 with:

$$F_h = \sqrt{1 - \frac{R}{a}} f_n \quad (7)$$

$$f_n = 1 + 0.358\lambda + 1.425\lambda^2 - 1.578\lambda^3 + 2.156\lambda^4, \ \lambda = R/a \quad (8)$$

89 and:

6

$$F_w = \sqrt{\sec\left(\frac{\pi R}{W}\right)\sec\left(\frac{\pi a}{W}\right)} \tag{9}$$

90 Observing equations (1), (2) and (6) it becomes clear why the 'characteristic

91 distance' l used in the average-stress model [6], which corresponds to the first

92 equation in (1), cannot be a material property: the geometric terms included in

93 the solution for the stress distribution, equation(2), and in the solution for the

94 stress intensity factor, equation (6), imply that the solutions of the system of

95 equations (1) are functions of both the geometry and the material properties.

96 The fact that the 'characteristic distance' is a function of the geometry of

97 the specimen has been demonstrated by several experimental results, see for

98 example [8].

99 Using (2) and (6) in (1), and dividing the second equation (1) by the square

100 of the first one yields:

$$\frac{4l\pi \int_R^{R+l} (F_h F_w)^2 \, a\,da}{R_K^2 \left\{\int_R^{R+l} \left[2 + \xi^2 + 3\xi^4 - (K_T^\infty - 3)(5\xi^6 - 7\xi^8)\right] dx\right\}^2} = \left(\frac{\mathcal{K}_{Ic}}{X_T^L}\right)^2 \tag{10}$$

101 The integral in the denominator of equation (10) can be solved analytically,

102 whereas the integral in the numerator cannot. Using Simpson's rule [25] to

103 numerically integrate the numerator of (10) the resulting non-linear equation

104 can be solved for l. Once l is known, it is possible to calculate the remote

105 stress at failure, $\bar{\sigma}^\infty$, using one of the equations (1).

106 It should be noted that the correction factors applied to the stress intensity

107 factor should account for the orthotropy of the composite material [26]. How-

108 ever, for quasi-isotropic laminates the stress intensity factor calculated using

109 (6) is accurate and no additional correction factors are required.

7

3 Material selection and characterization

The material selected for this work is the Hexcel IM7-8552 carbon epoxy unidirectional laminate. After laying-up, the material was cured according to the manufacturer's specifications, with temperature stages of 110°C during 1 hour, followed by 180°C for 2 hours using heating and cooling rates of 3°C/min. The pressure of 7 bar was applied during the duration of the curing cycle. To validate the finite fracture mechanics model using previously obtained experimental data [5] the $[90/0/\pm45]_{3s}$ lay-up is selected, corresponding to laminates with a nominal thickness of 3mm.

The finite fracture mechanics model proposed requires information about the laminate lay-up, the ply elastic properties, the laminate unnotched strength and the laminate mode I fracture toughness.

The ply elastic properties were measured in a previous investigation [5] using ASTM standards [27]-[28]. The results are shown in Table 1, where E_1 and E_2 are respectively the ply longitudinal and transverse Young's modulus, G_{12} is the ply shear modulus, and ν_{12} is the ply major Poisson's ratio. Table 1 also shows the standard used in each test, as well as the standard deviation (STDV).

[Table 1 about here.]

The unnotched tensile strength of the laminate, X_T^L, was measured using five test specimens. The tests were performed following the ASTM standard D-3039 [27], and the average value obtained was $X_T^L = 845.1$MPa (standard deviation of 47MPa).

8

There are no standard test methods to measure the fracture toughness of the laminate. Taking into account the simplicity of the geometry and of the data reduction method, specimens with a central crack are selected to measure this property.

Four specimens with central cracks with a length $2a = 15$mm were tested. Two of the test specimens are 45mm wide and the other two are 48mm wide. The specimens were loaded in tension at a rate of 2mm/min until final failure. All the specimens tested failed by net-tension, with crack propagation from the original central crack towards the edges of the specimen.

The calculation of the fracture toughness is based on the finite fracture mechanics analysis of the specimen with a central crack. Failure occurs when the following system of equations is satisfied:

$$
\begin{cases}
\frac{1}{l} \int_a^{a+l} \sigma_{yy}(x,0)dx = X_T^L \\
\\
\\
\frac{1}{l} \int_a^{a+l} \mathcal{K}_I^2(a)da = \mathcal{K}_{Ic}^2
\end{cases}
\tag{11}
$$

For sufficiently large W/a ratios, the stress distribution used in equation (11) reads:

$$
\sigma_{yy}(x,0) = \frac{\sigma^\infty x}{\sqrt{x^2 - a^2}}
\tag{12}
$$

and the stress intensity factor is given by:

9

$$\mathcal{K}_I = \sigma^\infty \sqrt{\pi a} \qquad (13)$$

Using the remote stress at failure measured in the experimental tests of the cracked specimens, $\bar{\sigma}^\infty$, and knowing the laminate unnotched strength, $X_T^L = 845.1$MPa, it is possible to solve (11) for $\mathcal{K}_{Ic}$ and for l. Following this procedure, the mean value of the fracture toughness is 48.0MPa$\sqrt{\text{m}}$ (standard deviation of 1.6MPa$\sqrt{\text{m}}$).

It is interesting to note that this value is quite close to that obtained from the direct application of Linear-Elastic Fracture Mechanics (45.1MPa$\sqrt{\text{m}}$). This means that it is possible to use models that relate the fracture toughness of the 0° ply to the fracture toughness of a multidirectional laminate [29] in the finite fracture mechanics model without incurring in significant errors.

4   Model validation

The model proposed in this paper is validated by comparing its predictions with experimental data obtained in IM7-8552 CFRP open-hole tensile tests [5],[21].

Open-hole tensile tests were performed in a previous investigation using the $[90/0/\pm45]_{3s}$ lay-up [5]. Specimens with five different hole diameters, $d=2$mm, 4mm, 6mm, 8mm, 10mm and with a constant width-to-diameter ratio (W/d) equal to 6 were tested following the ASTM D-5766 standard [30]. All the details of the tests performed and the test results are presented in [5].

The comparison between the experimental results and the predictions of the

10

168 finite fracture mechanics (FFM) previously described is shown in Figure 2

169 and in Table 2. The comparison includes the predictions obtained using the

170 point stress (PS) model [6], which requires the inverse identification of the

171 'characteristic distance'. Using the test results of the specimen with a 6mm

172 diameter hole the characteristic distance is calculated as 0.83mm.

173 [Fig. 2 about here.]

174 [Table 2 about here.]

175 The results shown in Figure 2 and in Table 2 indicate that the finite fracture

176 mechanics model provides more accurate predictions than the point stress

177 model. In addition, it should be stressed that, unlike the point stress model,

178 the finite fracture mechanics model does not require any inverse identification

179 from one of the tests.

180 To further validate the model proposed in this paper, additional experimen-

181 tal information on the open hole tensile strength of laminates manufactured

182 using the same material system, Hexcel IM7-8552, is used. Green et al. [21]

183 performed tests using the $[45/90/-45/0]_{4s}$ lay-up, with W/d=5 and hole di-

184 ameters equal to 3.175mm, 6.35mm, 12.7mm, and 25.4mm. The unnotched

185 strength reported for this lay-up is $X_T^L = 929$MPa [31]. However, there is no

186 information regarding the mode I fracture toughness of this lay-up, a property

187 required for the finite fracture mechanics model.

188 To estimate the value of $\mathcal{K}_{Ic}$ the results of the test performed in the specimen

189 with a 3.175mm hole is used. Knowing the unnotched strength of the material

190 and the notched strength of this test specimen it is possible to solve equation

191 (1) for l and $\mathcal{K}_{Ic}$, which results in $\mathcal{K}_{Ic} = 42.3$MPa$\sqrt{\text{m}}$. This value is close to

11

192 that experimentally obtained for the $[90/0/\pm 45]_{3\mathrm{s}}$ lay-up.

193 Equipped with this value, it is now possible to predict the notched strength for

194 the other geometries. The comparison between the experimental results and

195 the predictions is shown in Figure 3 and in Table 3. The comparison includes

196 the predictions obtained using the point stress (PS) model with a characteristic

197 distance of 0.45mm calculated using the specimen with a 3.175mm diameter

198 hole.

199 [Fig. 3 about here.]

200 [Table 3 about here.]

201 As before, improved results are obtained using the finite fracture mechanics

202 model.

203 Taking into account that the finite fracture mechanics model provides predic-

204 tions of notched strength in a few of seconds, it can be used to generate design

205 charts for notched laminates. Figure 4 shows the predicted normalized notched

206 strength of the $[90/0/\pm 45]_{3\mathrm{s}}$ laminate, defined as $\bar{\sigma}_N = \bar{\sigma}^\infty / X_T^L$, as a function

207 of the d/W ratio for different hole sizes. This Figure also includes the predic-

208 tions obtained for a notch-sensitive material, whose normalized strength is a

209 function of the stress concentration factor K_T ($\bar{\sigma}_N = 1/K_T$), and the predic-

210 tions for a notch-insensitive material, whose normalized strength is a function

211 of the geometry ($\bar{\sigma}_N = 1 - d/W$).

212 [Fig. 4 about here.]

213 Figure 4 shows that, for a constant d/W ratio, the finite fracture mechanics

214 model predicts that the mechanical response of a notched composite laminate

12

215 moves from notch sensitivity to notch insensitivity for decreasing hole sizes.

216 This result is consistent with the experimental results previously presented.

217 In addition, the finite fracture mechanics model predicts that for large d and

218 d/W ratios the response becomes brittle and a simple analysis based on stress

219 concentration factors would yield sufficiently accurate predictions.

220 To further illustrate how the finite fracture mechanics model can be used to

221 assess the inherent brittleness of a given material and geometry, the following

222 notch sensitivity factor is introduced:

$$\eta_N = \frac{d}{l} \tag{14}$$

223 where l is calculated from the non-linear equation (10). This notch sensitivity

224 factor is equivalent to the dimensionless group introduced by Suo et al. [32] in

225 terms of the notch size, the material Young's modulus and unnotched strength,

226 and the crack opening displacement.

227 The finite fracture mechanics model is used to predict the notch sensitivity

228 factor of the IM7-8552 $[90/0/\pm45]_{3s}$ laminate with $W/d = 6$ using two ad-

229 ditional extreme cases. The first one correspond to a ductile material with

230 a fracture toughness corresponding to twice that calculated for IM7-8552

231 $[90/0/\pm45]_{3s}$ ($\mathcal{K}_{Ic}=2\times48.0\mathrm{MPa}\sqrt{\mathrm{m}}$); the second case corresponds to a brittle

232 material with a fracture toughness corresponding to one-half of that previously

233 used ($\mathcal{K}_{Ic}=1/2\times48.0\mathrm{MPa}\sqrt{\mathrm{m}}$).

234 Figure 5 shows the relation between the notch sensitivity factor and the hole

235 diameter for the three materials considered and Figure 6 shows the corre-

236 sponding predicted relation between the hole diameter and the normalized

237 strength.

238   [Fig. 5 about here.]

239   [Fig. 6 about here.]

240 The previous figures demonstrate that the model developed in this work is use-

241 ful to assess the inherent brittleness of a given material/geometry combination.

242 The notch sensitivity factor increases with the hole size, specially for materials

243 with a low fracture toughness. For the materials and geometries used in this

244 example it is concluded that when $\eta_N \geq 22.5$ (brittle material/structure) it

245 is possible to predict the notched strength with a good accuracy simply using

246 the stress concentration factor as: $\bar{\sigma}^\infty = X_T^L/K_T$. Figure 6 shows that in such

247 conditions the finite fracture mechanics prediction tends to the solution ob-

248 tained for a perfectly brittle, notch sensitive material. When $\eta_N \leq 0.4$ (ductile

249 material/structure) it is possible to predict the notched strength simply using

250 the geometry of the specimen as: $\bar{\sigma}^\infty = X_T^L (1 - d/W)$. More complex analysis

251 methods are required for the intermediate, quasi-brittle, material response.

252 **5   Conclusions**

253 The finite fracture mechanics model developed in this paper is an economic,

254 fast and accurate method to predict the open-hole tensile strength of com-

255 posite laminates. Economic because it only requires the ply elastic constants

256 and two additional independent material properties: the laminate unnotched

257 strength and the laminate fracture toughness. No inverse identification meth-

258 ods are required. The predictions are obtained in a few seconds because no

259 finite element analysis or complex computational methods are required. Fi-

14

₂₆₀ nally, based on the comparison between the predictions and the experimental

₂₆₁ results, it is concluded that the finite fracture mechanics model is very accu-

₂₆₂ rate.

₂₆₃ These characteristics of the model make it quite suitable for the generation of

₂₆₄ design charts for notched composite laminates, to predict the notch sensitivity

₂₆₅ of a given material/structure, and to verify when simple strength of materials

₂₆₆ analysis are suitable design tools.

₂₆₇ The finite fracture mechanics model is applicable to notched composite lam-

₂₆₈ inates that exhibit either brittle or pull-out failure modes. The strength pre-

₂₆₉ diction of laminates whose main failure mechanism is delamination requires

₂₇₀ appropriate finite element analysis; the model proposed herein is not appro-

₂₇₁ priate for this type of laminates.

₂₇₂ Future work will address the generalization of the model to deal with the

₂₇₃ strength prediction of notched composite laminates subjected to multi-axial

₂₇₄ loading.

References

[1] Wisnom MR. Modelling discrete failures in composites with interface elements. Composites Part A: Applied Science and Manufacturing 2010;41(7):795-805.

15

[2] Tay TE, Tan SHN, Tan VBC, Gosse JH. Damage progression by the element-failure method (EFM) and strain invariant failure theory (SIFT). Composites Science and Technology 2005;65(6):935-944.

[3] van der Meer FP, Oliver C, Sluys LJ. Computational analysis of progressive failure in a notched laminate including shear nonlinearity and fiber failure. Composites Science and Technology 2010;70(4):692-700.

[4] Laurin F, Carrère N, Maire JF. A multiscale progressive failure approach for composite laminates based on thermodynamical viscoelastic and damage models. Composites-Part A 2007;38:198-209.

[5] Camanho PP, Maimí P, Dávila CG. Prediction of size effects in notched laminates using continuum damage mechanics. Composites Science and Technology 2007;67:2715-2727.

[6] Whitney JM, Nuismer RJ. Stress fracture criteria for laminated composites containing stress concentrations. Journal of Composite Materials 1974; 8:253-265.

[7] Chang, FK, Scott, RA, Springer, GS. Strength of mechanically fastened composite joints. Journal of Composite Materials 1982;16:470-494.

[8] Camanho PP, Lambert M. A design methodology for mechanically fastened joints in laminated composite materials. Composites Science and Technology 2006;66:3004-3020.

[9] Bäcklund J. Fracture analysis of notched composites. Computers & Structures 1981;13:145-154.

[10] Aronsson CG, Bäcklund J. Tensile fracture of laminates with cracks. Journal of Composite Materials 1986;20:287-307.

[11] Bäcklund J, Aronsson CA. Tensile fracture of laminates with holes. Journal of Composite Materials 1986;20:259-286.

16

[12] Carlsson LA, Aronsson CG, Bäcklund J. Notch sensitivity of thermoset and thermoplastic laminates loaded in tension. Journal of Materials Science 1989;24:1670-1682.

[13] Leguillon D. Strength or toughness? A criterion for crack onset at a notch. European Journal of Mechanics A/Solids 2002;21:61-72.

[14] Cornetti P, Pugno N, Carpinteri A, Taylor D. Finite fracture mechanics: A coupled stress and energy failure criterion. Engineering Fracture Mechanics 2006;73:2021-2033.

[15] Andersons J, Tarasovs S, Sparnins E. Finite fracture mechanics analysis of crack onset at a stress concentration in a UD glass/epoxy composite in off-axis tension. Composites Science and Technology 2010;70:1380-1385.

[16] Hebel J, Dieringer R, Becker W. Modelling brittle crack formation at geometrical and material discontinuities using a finite fracture mechanics approach. Engineering Fracture Mechanics 2010;77:3558-3572.

[17] Carpinteri A, Cornetti P, Pugno N, Sapora A, Taylor D. A finite fracture mechanics approach to structures with sharp V-notches. Engineering Fracture Mechanics 2008;75:1736-1752.

[18] Taylor D, Cornetti P, Pugno N. The fracture mechanics of finite crack extension. Engineering Fracture Mechanics 2005;72:1021-1038.

[19] Müller A, Becker W, Stolten D, Hohe J. A hybrid method to assess interface debonding by finite fracture mechanics. Engineering Fracture Mechanics 2006;73:994-1008.

[20] Martin E, Leguillon D, Carrère N. A twofold strength and toughness criterion for the onset of free-edge shear delamination in angle-ply laminates. International Journal of Solids and Structures 2010;47:1297-1305.

17

[21] Green BG, Wisnom MR, Hallet SR. An experimental investigation into the tensile strength scaling of notched composites. Composites-Part A 2007;38:867-878.

[22] Tan SC. Stress concentrations in laminated composites. Technomic, 2004.

[23] Newman JC Jr. A nonlinear fracture mechanics approach to the growth of small cracks. In: Proceedings of AGARD Conference 1983;328(6).

[24] Tsai SW, Ha S, Tay TE, Miyano Y, Sihn S. Strength & Life of Composites. In: Tsai SW, editor. U.S.A. Aeronautics & Astronautics, Stanford University, 2008.

[25] Kreyszig E. Advanced Enginnering Mathmathics. John Wiley and Sons, 1993.

[26] Bao G, Ho S, Suo Z, Fan B. The role of material orthotropy in fracture specimens for composites. International Journal of Solids and Structures 1992;29:1105-1116.

[27] Standard test method for tensile properties of polymer matrix composite materials, ASTM D 3039/D 3039M-00. American Society for Testing and Materials (ASTM). West Conshohocken, PA, U.S.A.

[28] Standard test method for in-plane shear response of polymer matrix composite materials by test of a $\pm45\,^\circ$ laminate, ASTM D 3518/3518M-94. American Society for Testing and Materials (ASTM). West Conshohocken, PA, U.S.A.

[29] Camanho PP, Catalanotti G. On the relation between the composite laminate fracture toughness and that of the $0°$ ply fracture toughness: analytical model and experimental validation. Engineering Fracture Mechanics 2011;78:2535-2546.

[30] Open hole tensile strength of polymer composite laminates, ASTM D 5766/D 5766M-02a. American Society for Testing and Materials (ASTM). West Conshohocken, PA, U.S.A.

18

[31] Wisnom M, Khan B, Hallett S. Size effects in unnotched tensile strength of unidirectional and quasi-isotropic carbon/epoxy composites. Composite Structures 2008;84:21-28.

[32] Suo Z, Ho S, Gong X. Notch ductile-to-brittle transition due to localized inelastic band. J. of Engineering Materials and Technology 1993;115: 319-326.
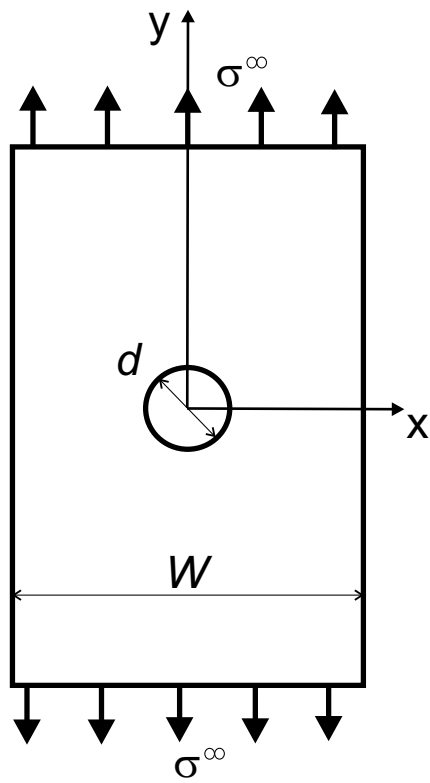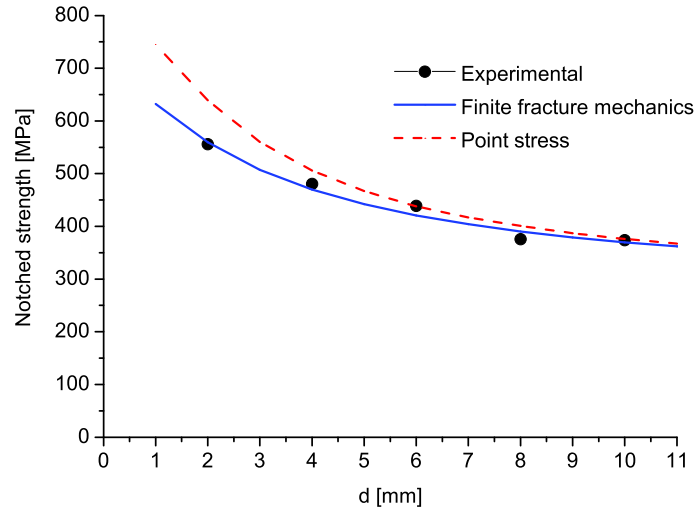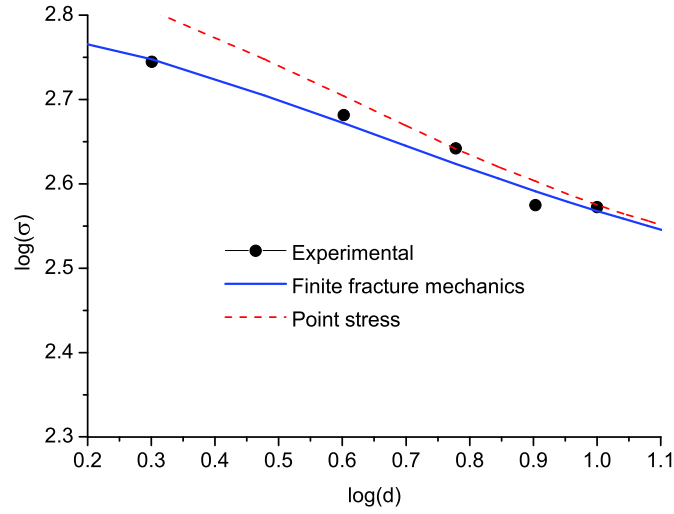
List of Figures

Fig. 1. Notched laminate under tensile loading.
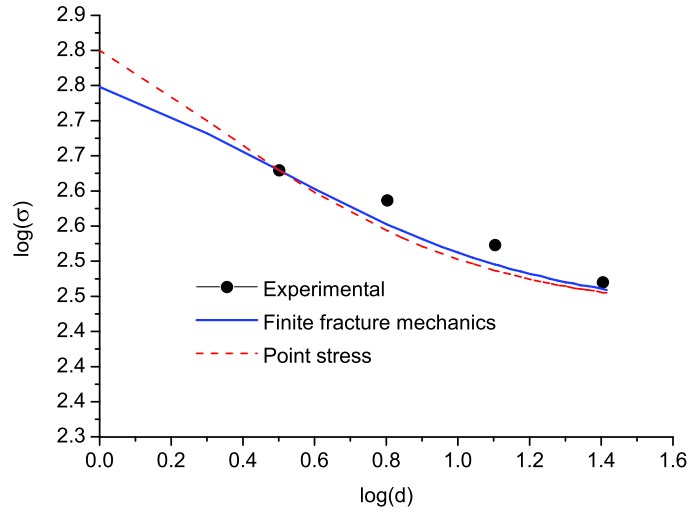
(a) Notched strength vs. hole diameter.

(b) Notched strength vs. hole diameter (logarithmic scale).

Fig. 2. Comparison between predictions and experiments - $[90/0/\pm 45]_{3s}$ lay-up.
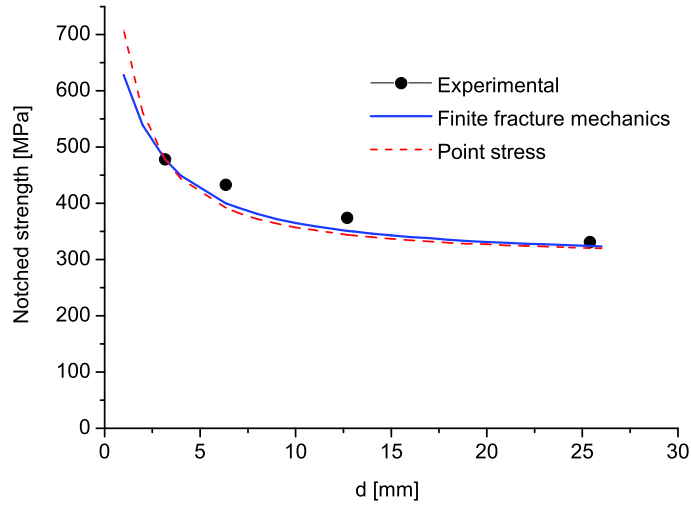
(a) Notched strength vs. hole diameter.

(b) Notched strength vs. hole diameter (logarithmic scale).

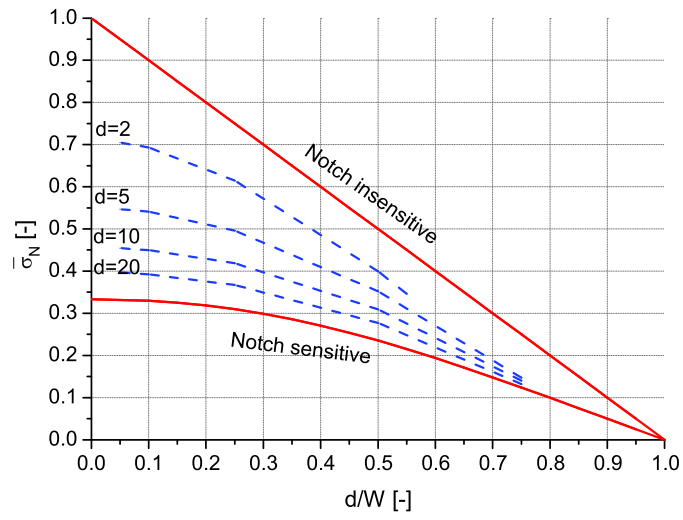Fig. 3. Comparison between predictions and experiments - $[45/90/-45/0]_{4s}$ lay-up.

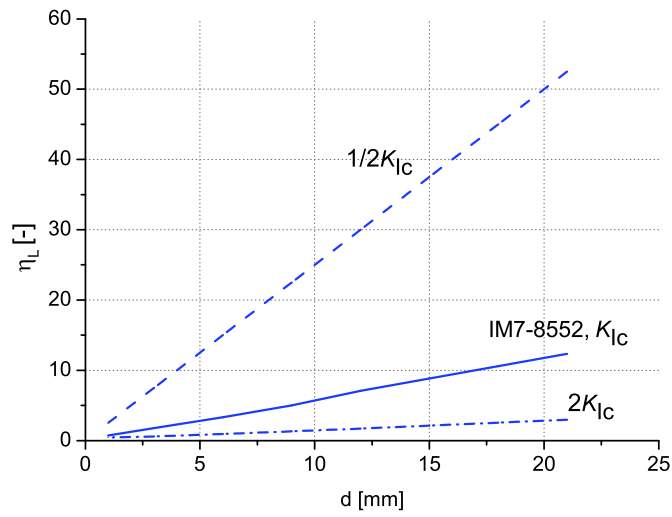Fig. 4. Design chart for IM7-8552 $[90/0/\pm 45]_{3s}$ laminates.

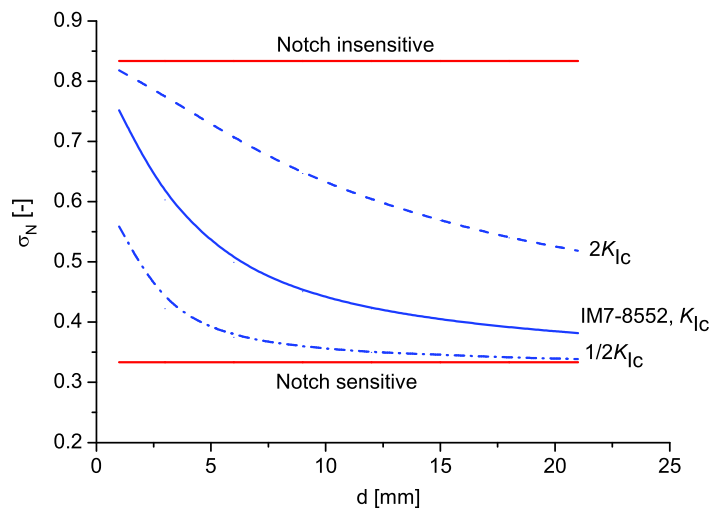Fig. 5. Notch sensitivity factor calculated using finite fracture mechanics.

Fig. 6. Predicted normalized strength for different materials.

List of Tables

Table 1

Ply elastic properties.

Property	Standard	Mean value	STDV
E_1 [GPa]	Ref. [27]	171.4	2.38
E_2 [GPa]	Ref. [27]	9.1	0.09
G_{12} [GPa]	Ref. [28]	5.3	0.13
ν_{12}	Ref. [27]	0.3	0.02

Table 2

Comparison between predictions and experiments for the $[90/0/\pm 45]_{3s}$ lay-up.

d [mm]	$\bar{\sigma}^\infty$ (Exp.) [MPa]	$\bar{\sigma}^\infty$ (FFM) [MPa]	Error (%)	$\bar{\sigma}^\infty$ (PS) [MPa]	Error (%)
2	555.7	560	+0.7	639	+15.0
4	480.6	470	-2.2	506	+5.3
6	438.7	420	-4.1	n/a	n/a
8	375.7	390	+3.8	401	+6.7
10	373.7	370	-1.1	376	+0.6

Table 3

Comparison between predictions and experiments for the $[45/90/-45/0]_{4s}$ lay-up.

d [mm]	$\bar{\sigma}^{\infty}$ (Exp.) [MPa]	$\bar{\sigma}^{\infty}$ (FFM) [MPa]	Error (%)	$\bar{\sigma}^{\infty}$ (PS) [MPa]	Error (%)
3.175	478	n/a	n/a	n/a	n/a
6.35	433	400	-7.6	392	-9.5
12.7	374	351	-6.1	344	-8.0
25.4	331	324	-2.1	320	-3.3